Superfluorescence-Stimulated Photon Echoes

A. I. Lvovsky,[1,3,*] S. R. Hartmann,[1] and F. Moshary[2]

[1]*Department of Physics, Columbia University, New York, New York 10027*
[2]*Department of Electrical Engineering, City College of New York, New York, New York 10031*
[3]*Fachbereich Physik, Universität Konstanz, D-78457 Konstanz, Germany*
(Received 4 June 2002; published 10 December 2002)

Two closely spaced 778 nm, 4-ps pulses, two-photon resonant with the $5S - 5D$ transition in Rb vapor generate a ground state grating, which later is excited by a similar third pulse, producing conical yoked superfluorescence echo on the $5S - 6P$, 420-nm transition. The intensity of this emission as a function of the relative delay between the leading excitation pulses is governed by the dynamics of Doppler dephasing and rephasing. This is the first observation of an echo effect induced by a spontaneous relaxation process.

Photon echo is a coherent optical emission resulting from reversal of inhomogeneous dephasing in a medium excited by a sequence of laser pulses. Since its first observation in 1964 [1], photon echo has developed into a powerful scientific tool with a wide range of applications in spectroscopy [2], holographic optical storage, and optical signal processing [3]. Recently, the phenomenon has raised a new wave of interest due to a possible application for quantum information processing and storage [4].

It is commonly accepted that all homogeneous relaxation processes, in particular, spontaneous emission, reduce the coherence present in the medium and, thus, degrade the echo magnitude. In this Letter, we show this view to be only partially correct. If spontaneous relaxation is *coherent,* such as in the case of superfluorescence, it may not just preserve the echo, but generate it, playing the role of one of the excitation pulses. We investigate a photon echo-type of effect stimulated by superfluorescence and find it to possess a unique set of properties.

Superfluorescence (SF) is observed in ensembles of two-level dipoles prepared with sufficient population inversion. If the optical gain is very high, spontaneous emission develops a macroscopic transition moment, resulting in depletion of the upper state in a time much faster than the spontaneous lifetime of the system. A burst of coherent radiation ensues and the population is transferred coherently to the lower level.

In the present work, SF occurs on the $5D - 6P$ transition in atomic vapor of rubidium following a two-photon excitation from the ground level $5S$ (Fig. 1). The sample is excited in a large Fresnel number (quasispherical) configuration and the optical gain is on the order of 10^4. Under these conditions, superfluorescence obtains *omnidirectional* character [5]. Spontaneously emitted photons are amplified and generate a set of randomly phased dipole antennas distributed throughout a 4π solid angle, each antenna producing superfluorescent emission in its own direction.

Upon the onset of superfluorescence, the coherent superposition between levels $5S$ and $5D$ created by the laser excitation is transferred to the $6P - 5S$ transition. This transition is dipole allowed and will generate a coherent optical pulse along all wave vectors that satisfy the phase-matching condition. This phenomenon is known as *yoked* superfluorescence (YSF) [6] and can be interpreted as four-wave mixing that occurs in the absence of (after) the pump pulses.

The echo-type phenomenon investigated in this Letter takes place when YSF is initiated from a $5S - 5S$ superposition ground state prepared by two laser pulses, each two-photon resonant with the $5S - 5D$ transition. The $6P - 5S$ yoked emission not only appears as a well collimated beam along $\vec{k}_3$ (where $\vec{k}_i$ are the wave vectors of the three excitation pulses), but also as a conical distribution whose axis is tilted from $\vec{k}_3$ by $\vec{k}_2 - \vec{k}_1$. Unlike the emission along $\vec{k}_3$, this conical emission is strongly dependent on the order and angular and temporal separation of the first two pulses. Although very different, there are striking similarities between this effect and the common stimulated photon echo involving single-photon transitions. These similarities lead us to interpret the conical emission as a superfluorescence-stimulated virtual photon echo (SFSE): it is generated by, and simultaneous with, the omnidirectional SF that takes place on the upper leg of the $5D - 6P - 5S$ transition.

As is well known, the normal stimulated echo manifests itself as a well collimated beam that is displaced
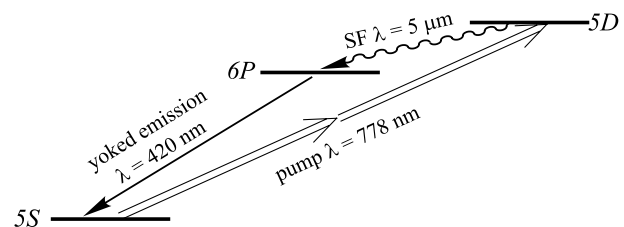
FIG. 1. Energy level diagram of yoked superfluorescence in atomic rubidium.

from $\vec{k}_3$ in like manner as the axis of the conical emission we observe here. Both in conventional and SF-stimulated echoes, the first two pulses generate a population grating, but whereas the normal stimulated echo can be interpreted as *scattering* of the third pulse off this grating, the superfluorescent echo cannot. In SFSE, the scattering is mediated by omnidirectional superfluorescence, so the echo pulse is emitted at a wavelength not equal to that of the excitation pulses nor their linear combination.

In the normal stimulated echo, the third pulse generates a superposition state which grows (rephases) and then decays (dephases) with the characteristic time scale T_2^*, the inhomogeneous relaxation time. The echo intensity follows this envelope and is maximized at $t_3 + t_2 - t_1$, where t_i denotes the time of arrival of the excitation pulses. In our experiment, on the other hand, the third pulse triggers YSF at a time $t_3 + \tau_{SF}$, where τ_{SF} is the SF delay time. The YSF and the $P - S$ superposition state it creates are *short lived* and neither grow nor decay. The intensity of SFSE depends on when they are triggered, i.e., τ_{SF} relative to $t_2 - t_1$, and peaks at τ_{SF} equal to $t_2 - t_1$ when YSF occurs at the same time the inhomogeneous rephasing of the $P - S$ superposition is at its maximum. We call SFSE "virtual" as we detect only a portion of the rephasing envelope at the time $t = t_3 + \tau_{SF}$ when the upper state SF ensues.

The ground state superposition (population grating) produced by the first two pulses has wave vector $2(\vec{k}_1 - \vec{k}_2)$ (the factor of 2 is because our excitation pulses are two-photon resonant). In addition, since the pulses are intense, any generated excited state grating quickly depopulates via $5D - 6P$ superfluorescence. By the time of arrival of the third pulse, $5S$ is the only populated level. The third pulse immediately creates a $5S - 5D$ coherence phased along $2\vec{k}_3$, as well as along $2(\vec{k}_3 + \vec{k}_2 - \vec{k}_1)$ and $2(\vec{k}_3 + \vec{k}_1 - \vec{k}_2)$. After a delay, τ_{SF}, omnidirectional superfluorescence, directed along a spherical set $\{\vec{k}_u\}$, ensues on the upper $6P - 5D$ transition, generating a yoked $5S - 5P$ coherence on the lower transition which emits along the set $\{\vec{k}_l\}$. This set is constrained by the wave vector matching condition. YSF is observed along the expected channel in the direction of the third pulse $2\vec{k}_3 = \vec{k}_u + \vec{k}_l$ ($\vec{k}_u$ and $\vec{k}_l$ collinear with $\vec{k}_3$). Additionally, because of the omnidirectional character of the upper transition superfluorescence, the ground state grating makes other simultaneous YSF channels possible under geometries that satisfy either

$$\vec{k}_u + \vec{k}_l = 2[\vec{k}_3 + (\vec{k}_2 - \vec{k}_1)] \tag{1a}$$

or

$$\vec{k}_u + \vec{k}_l = 2[\vec{k}_3 + (\vec{k}_1 - \vec{k}_2)] \tag{1b}$$

wave matching conditions.

At most, only one of the above two relations can be satisfied for a given excitation pulse geometry. By convention, we define pulses 1 and 2 so that it is the former equation that can be satisfied and hereafter we limit the discussion to that relation. If pulse 2 arrives earlier than pulse 1, we say that the delay $\Delta t = t_2 - t_1$ of pulse 2 is negative. Equation (1a) is, in fact, satisfied by a set of directions $\{\vec{k}_u + \vec{k}_l\}$, such that the emission associated with $\{\vec{k}_l\}$ is conical with its axis lying along $\vec{k}_3 + (\vec{k}_2 - \vec{k}_1)$ and its apex angle, 2θ, being determined by the three laser excitation directions:

$$\cos\theta = \frac{4k^2 + (4k\sin\alpha)^2 - 16k^2\sin\alpha\cos\phi + k_l^2 - k_u^2}{2k_l\sqrt{4k^2 + (4k\sin\alpha)^2 - 16k^2\sin\alpha\cos\phi}}, \tag{2}$$

where 2α is the angle between $\vec{k}_1$ and $\vec{k}_2$, ϕ is the angle between $\vec{k}_3$ and $\vec{k}_2 - \vec{k}_1$, and $k = |\vec{k}_1| = |\vec{k}_2| = |\vec{k}_3|$ is the laser wave number.

The above equation has a solution when $\phi \leq \pi/2 - \alpha$ or

$$|\vec{k}_u| + |\vec{k}_l| \geq 2|\vec{k}_3 + (\vec{k}_2 - \vec{k}_1)|. \tag{3}$$

For $\phi = \pi/2 - \alpha$, (3) becomes an equality and the cone collapses into a beam ($\theta = 0$) along $2\vec{k}_3 - 2\vec{k}_1 + 2\vec{k}_2$. This is the case when the three pulses enter the sample along the three legs of a pyramid with a rectangular base. The echo pulse is then emitted along the fourth leg. This (or similar) geometry is optimal for conventional stimulated photon echo/transient grating experiments, as only with this configuration is perfect phase-matching achieved [7]. On the other hand, conical SFSE is observed in a variety of geometries, as long as the inequality (3) stays valid.

The spatial properties of the SFSE, as described above, permit exact experimental verification. We used a Spectra-Physics Ti:sapphire mode locked laser/ regenerative amplifier system tuned to the two-photon resonance with the $5S - 5D$ Rb transition ($\lambda = 778$ nm). It generated 4-picosecond, 0.5-millijoule pulses at a 1 kHz repetition rate. The laser output was split into three 0.5-cm diameter beams of approximately equal intensity, and the beams were angled and spatially overlapped in a 1-cm-long quartz cell containing saturated vapor of rubidium. The cell was placed in an oven and heated to 140–160 °C. The relative delay of each pulse could be varied.

The YSF pulses on the lower $6P - 5S$ (420 nm) transition generated by the sample were separated from the pump laser by means of two narrow band interference filters and observed with a Sony XC-77 CCD camera. The camera was placed behind the oven facing the beams, with its 25-mm objective lens tuned to infinity so that the CCD array plane coincided with the Fourier plane of the lens.

The photograph shown in Fig. 2(a) was taken at a small ($t_2 - t_1 < 100$ ps) positive value of the relative pulse delay, and the third pulse delayed from the first pulse by

(a)

(b)
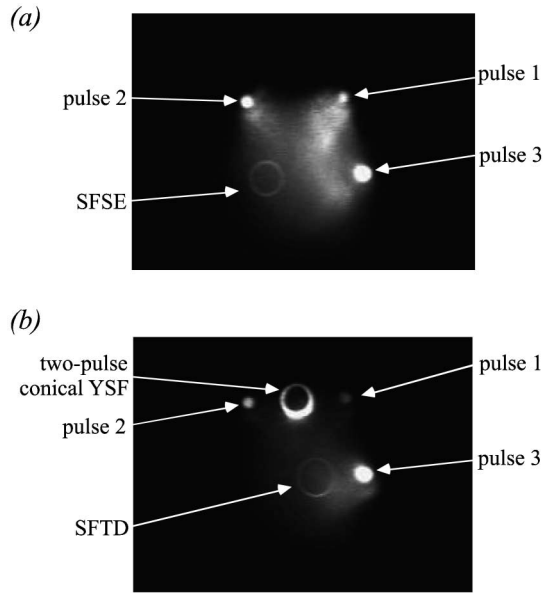
FIG. 2.   A photograph of the lower leg YSF emission. Conical YSF shows as a ring; also visible are the spots associated with the three YSF pulses generated by each laser beam alone. (a) Superfluorescence echo, $\Delta t \neq 0$; (b) transient diffraction off a two-photon grating, $\Delta t = 0$. Also visible in (b) is the cone of the two-pulse YSF described in [5].

$t_3 - t_1 = 5.5$ ns. The SFSE cone is clearly distinguishable. It disappeared if one of the three excitation pulses was blocked. When $t_2 - t_1 = 0$, the picture changes to that shown in Fig. 2(b). The rings visible in this picture are the two-photon conical YSF [5] and *superfluorescent transient diffraction* (SFTD) off the $\vec{k}_1 - \vec{k}_2$ grating (as opposed to the $2\vec{k}_1 - 2\vec{k}_2$ grating in the case of SFSE). This grating is created as a result of a combination of a photon absorption from pulse 1 and stimulated emission into pulse 2 and takes place only when pulses 1 and 2 are applied simultaneously. The resulting emission is conical with the symmetry axis along $2\vec{k}_3 - \vec{k}_1 + \vec{k}_2$ and apex angle η dependent on α and ϕ.

In Fig. 3, the theoretical (2) and experimental dependencies of θ and η on ϕ for a fixed $\alpha = 18.8$ mrad are displayed, showing good agreement with each other. All angles were determined by the camera which had a 0.55 mrad pixel resolution.

We have studied the dependence of the SFSE signal intensity (I_e) on the temporal separation $t_2 - t_1$ and $t_3 - t_1$ between the excitation pulses. The variation of $t_3 - t_1$ in the range of 1–15 ns showed little to no effect on the magnitude of the echo signal. This is not surprising as relaxation of the ground state grating is very slow. On the other hand, the effect of the second pulse delay is quite dramatic. Although there is no theoretical model that would accurately describe the behavior of I_e as a function of $t_2 - t_1$, its major features can be well understood on a qualitative level.
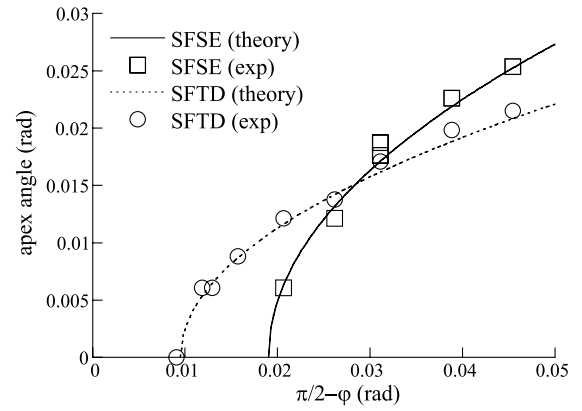
FIG. 3.   Apex angles 2θ and 2η of the conical YSF shown in Fig. 2(a) and 2(b) plotted as a function of $\pi/2 - \phi$, where $\phi = \angle(\vec{k}_3, \vec{k}_1 - \vec{k}_2)$ for a fixed $\alpha = (1/2)\angle(\vec{k}_1, \vec{k}_2) = 18.8$ mrad. Theoretical and experimental results are shown.

The mechanics of the echo formation is best explained by using the heuristic billiard-ball model [8]. The ensemble of atoms in the sample is represented by a wave packet whose size is determined by the thermal distribution of atomic momenta. When a wave packet is exposed to a short optical pulse, it divides and recoils according to the momentum of the photon absorbed or emitted. Associated with overlapping wave packets is a macroscopic transition moment which can generate superradiant emission. By following the wave packet trajectories and noticing when they cross, one discovers the temporal properties of this emission. The wave packet trajectories are conveniently displayed in a recoil diagram which is an analog of Feynman diagrams and shows the wave packet center displacement as a function of time.

The recoil diagram corresponding to our experiment is shown in Fig. 4. The heavy trajectories show the $S - P$ superposition states which give rise to the conical emission. As seen from the figure, complete rephasing occurs
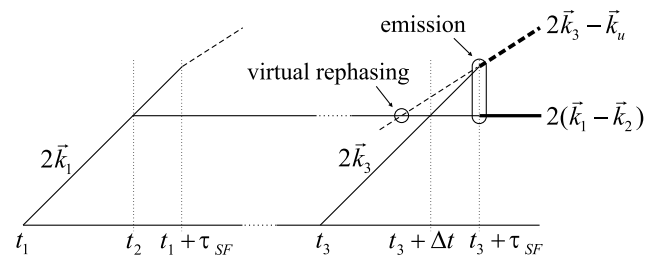
FIG. 4.   Recoil diagram showing trajectories that lead to the superfluorescence stimulated echo (Δt assumed positive). The $5S$ trajectory is represented by horizontal lines, $5D$ and $6P$ by solid and dashed slanted lines, respectively. The two-photon resonant laser excitation pulses are applied at t_1, t_2, t_3 with the omnidirectional superfluorescence taking place at $t_3 + \tau_{SF}$. The heavy trajectories show the $S - P$ superposition which gives rise to the echo emission. Excitation of atomic levels due to the pulse at time t_2 is not shown for simplicity.
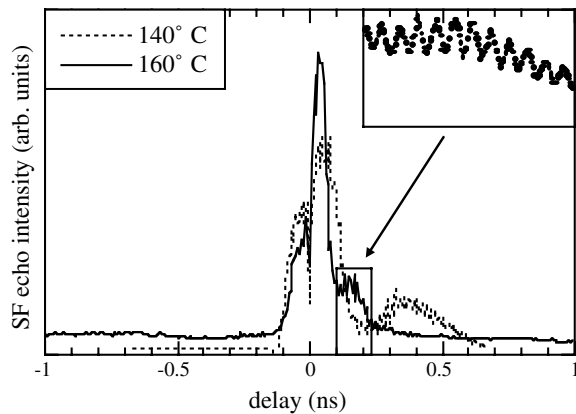
FIG. 5. Energy of the SFSE pulse as a function of the second pulse delay Δt.

before the $S - P$ superposition is formed and the emission can begin. The delay is minimized when Δt is just slightly smaller than τ_{SF}. The measured conical emission intensity corresponds to the integrated rephasing envelope over the very short ($\ll T_2^*$) lifetime of the YSF emission at $t_3 + \tau_{\mathrm{SF}}$, providing a snapshot of the $5S - 5D$ coherence at the moment the upper state SF ensues. Thus, the SFSE is at its maximum when the moment of complete rephasing coincides with the YSF emission, i.e., $\Delta t \approx \tau_{\mathrm{SF}}$. As Δt is decreased, the $2(\vec{k}_1 - \vec{k}_2)$ trajectory moves downwards, the YSF emission comes after the peak of Doppler rephasing, and SFSE becomes degraded by inhomogeneous dephasing. This trend continues for negative delays.

In order to investigate SFSE's temporal properties, the CCD camera was replaced by an EG&G C90302 avalanche photodiode connected to a Tektronix TDS 754A 500-MHz digital oscilloscope. The geometry was chosen so that $\phi = \pi/2 - \alpha$ and the SFSE cone collapsed into a single beam, which was focused on the sensitive area of the detector. Before entering the photodiode, the beam was spectrally and spatially filtered to reduce the leakage from the pump and YSF pulses along the laser excitation directions. The energy of the SFSE signal as a function of $t_2 - t_1$ is shown in Fig. 5. We see that the strong signals are observed only within a relatively small range of $t_2 - t_1$. This is readily explained by the requirement that the first two pulses must arrive within a time frame shorter than the upper transition superfluorescence delay time τ_{SF}. If the second (by order) pulse is applied after the $5D$ level populated by the initial pulse is already depleted by the SF, no grating will be formed. Direct measurements of τ_{SF} determined it to be 150 and 95 ps at 140 and $160\,^{\circ}$C, respectively, which is consistent with this inter-

pretation. The asymmetry of the plot with respect to $t_2 - t_1 = 0$ is explained by the dynamics of inhomogeneous dephasing/rephasing as discussed above.

As evidenced by this figure, there is nonzero SFSE at relatively large, positive values of $t_2 - t_1$. This can be explained by Burnham-Chiao oscillations [9] associated with the repopulation of the $5D$ level after the onset of SF. The signal in this region exhibits modulation with the 90 GHz frequency which equals the fine splitting of the $5D$ level. The dip at $t_2 - t_1 = 0$ is associated with a number of competing multiphoton processes that occur only when two excitation pulses are applied simultaneously [5]. Their result is to diminish the amplitude of the $2\vec{k}_1 - 2\vec{k}_2$ ground state grating.

In summary, we have investigated how omnidirectional yoked superfluorescence exposes coherent superposition previously induced in the ground state. The temporal properties of the emission are explained by the dynamics of inhomogeneous dephasing/rephasing so we identify the observed phenomenon as superfluorescence-stimulated virtual photon echo.

Superfluorescence echo has a number of properties which make it unique in the wide range of photon echo phenomena. First, it is generated by a spontaneous relaxation process (superfluorescence). Second, it is a result of two-photon resonant excitation. Third, its frequency is not equal to that of the generating laser pulses nor their linear combination. Fourth, it is emitted in a cone.

---

*Email address: Alex.Lvovsky@uni-konstanz.de

[1] N. A. Kurnit, I. D. Abella, and S. R. Hartmann, Phys. Rev. Lett. **13**, 567 (1964).

[2] See, for example, W. Demtröder, *Laser Spectroscopy: Basic Concepts and Instrumentation* (Springer, Berlin, 2002).

[3] V. V. Samartsev, Laser Phys. **8**, 1198 (1998).

[4] S. A. Moiseev and S. Kröll, Phys. Rev. Lett. **87**, 173601 (2001).

[5] A. I. Lvovsky, S. R. Hartmann, and F. Moshary, Phys. Rev. Lett. **82**, 4420 (1999).

[6] J. H. Brownell, X. Lu, and S. R. Hartmann, Phys. Rev. Lett. **75**, 3265 (1995).

[7] P. Hu, R. Leigh, and S. R. Hartmann, Phys. Lett. **40A**, 164 (1972).

[8] R. Beach, S. R. Hartmann, and R. Friedberg, Phys. Rev. A **25**, 2658 (1982); R. Friedberg and S. R. Hartmann, Phys. Rev. A **48**, 1446 (1993); A. I. Lvovsky and S. R. Hartmann, J. Phys. B **31**, 3997 (1998).

[9] D. C. Burnham and R. Y. Chiao, Phys. Rev. **188**, 667 (1969).